ELSEVIER

Engineering Analysis with Boundary Elements 26 (2002) 929–937

ENGINEERING ANALYSIS *with* BOUNDARY ELEMENTS

www.elsevier.com/locate/enganabound

Acoustic analysis with absorbing finite elements and far-field computations using free-space Green's functions

A.M. Al-Khaleefi[a,*], A. Ali[b], C. Rajakumar[c], L.F. Kallivokas[d]

[a]*Department of Civil Engineering, Kuwait University, P.O. Box 5969, Safat 13060, Kuwait*
[b]*ESAS, 15160 SE 54th Place, Bellevue, WA 98006, USA*
[c]*ANSYS, Inc., 275 Technology Drive, Canonsburg, PA 15317, USA*
[d]*Carnegie Mellon University, Pittsburgh, PA 15213, USA*

Received 5 July 2001; revised 8 January 2002; accepted 25 July 2002

Abstract

A family of absorbing-boundary finite elements (FEs) is recently developed for the acoustic time-harmonic, transient and modal analyses of problems having fluid domains of infinite extent. These elements can be easily 'glued' to the truncated exterior surface of an underlying FE mesh. The desirable characteristics of the absorbing elements are that they are local and produce banded symmetric element matrices. Since the use of the absorbing FEs reduces the size of the FE model through the premature truncation of the mesh, a post-processing procedure must be employed to obtain solutions far away from FE domain in the case of transient and time-harmonic analyses. In this paper free-space Green's functions are utilized, in the context of time-harmonic analysis, in association with the computed solutions at the exterior boundary where absorbing-boundary FEs are placed in order to compute pressure distribution outside the FE computational domain. The paper demonstrates that the computation of accurate pressure gradients at the absorbing-boundary element nodes plays a crucial role in obtaining accurate pressure solutions outside the FE computational domain.

Keywords: Absorbing-boundary finite element; Free-space Green's function; Harmonic analysis

1. Introduction

The use of absorbing boundary elements (BEs) at the truncated boundary of an infinite-domain acoustic problem results in a smaller FE model and thus efficient solution of the discretized equations. A family of acoustics absorbing BEs in two and three dimensions was developed [1–4] to be placed at the truncated boundary of an underlying FE mesh to solve wave equation in unbounded domains. These elements can be used in conjunction with structural and acoustic FEs to perform transient, time-harmonic, modal and fluid-structure interaction analyses. The elements are based on the second-order asymptotic expansion procedure and are shown to produce accurate solutions for a reasonable distance of placement of these elements. The absorbing elements are local and so they preserve the bandedness of the assembled matrices of the coupled FE-infinite element system. Furthermore, these elements produce symmetric coefficient matrices. These properties make them suitable for implementation in a general-purpose computer program.

This family of absorbing-boundary infinite elements was implemented in the ANSYS program [5] in the form of two surface elements FLUID129 and FLUID130. FLUID129 is a two-noded surface element for use in planar or axisymmetric situation along with the four-noded FE FLUID29 while FLUID130 is a four-noded surface element, collapsible to three-noded triangular element, to be used with the eight-noded ANSYS FE FLUID30 for three-dimensional (3D) wave propagation problems. The new additions to the element library of ANSYS are intended to model 2D, axisymmetric or 3D infinite regions, where the governing field equation is the scalar wave equation. The typical application field of the new elements is acoustics and the elements can be used for either time-domain or frequency-domain analysis (transient, harmonic, or eigenvalue analysis type).

The use of the absorbing-BEs allows the analysts to cut short the FE domain dramatically. However, often field

* Corresponding author. Tel.: +965-4817240; fax: +965-4817524.
E-mail address: khaleefi@civil.kuniv.edu.kw (A.M. Al-Khaleefi).

0955-7997/02/$ - see front matter
PII: S0955-7997(02)00071-1

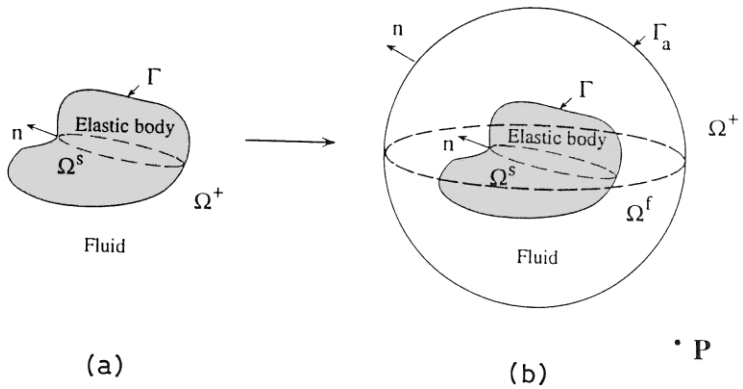

Fig. 1. Typical fluid-structure interaction geometry and absorbing boundary.

solutions are desired outside this truncated domain, especially in acoustic analysis. This paper demonstrates the use of integral equation in the computation of far-field pressure solutions in the context of time-harmonic analysis. To this end, the pressure solutions on the absorbing boundary are utilized. Note that the computation of pressure field using integral equation requires the pressure gradient values in addition to the pressure field on the absorbing boundary. The FE solution procedure computes pressure gradients by differentiating nodal pressure values and are not as accurate as the pressure solution. A simple but novel pressure gradient computation procedure is presented which uses the reactive nodal flows from the acoustics FEs attached to the absorbing elements, enforces global equilibrium at the nodes on the absorbing elements and recovers the pressure gradients.

The intent of the paper is to provide a presentation on the effectiveness of a combined computational process employing the BE and the FE concepts. There have been applications where BE–FE coupled analysis have been shown to be successfully applied to problems involving unbounded computational domain. The current approach, however, is different in using the BE computations as an effective post-processing methodology to calculate the far field acoustic pressures where the pressure solution obtained through FE computations is used. The advantage of this approach is, unlike the BE–FE coupled solution approach, the solution is performed using the FE approach where the matrices are symmetric and banded allowing the use of efficient solvers available in general purpose FE software packages.

In this paper, the theoretical foundation of the absorbing FEs is briefly summarized along with the implementation details of the absorbing FEs in the ANSYS program. The incorporation of the integral equation to compute far-field pressure in a planar frequency domain acoustic analysis is then described. 2D time-harmonic example problems in acoustics are presented to demonstrate the accuracy of the absorbing elements and the effectiveness of the free-space Green's functions in the computation of the far-field solutions.

2. Brief theory of absorbing elements

The exterior structural acoustics problem typically involves a structure submerged in an infinite, so-called acoustic fluid. The latter characterization implies that the fluid is homogeneous, linear, compressible and inviscid. When considering small barotropic disturbances of the pressure and density about an equilibrium state, it can be shown that the pressure field p within the fluid is described by the scalar wave equation as

$$\nabla^2 p = \frac{1}{c^2}\ddot{p} \qquad \text{in } \Omega^+ \tag{1}$$

where c is the speed of sound in the fluid, an overdot denotes derivative with respect to time and Ω^+ is the unbounded region occupied by the fluid (Fig. 1a). In addition to Eq. (1), Sommerfeld radiation condition, that simply states that the waves generated within the fluid are outgoing, needs to be satisfied at infinity. A primary difficulty associated with the use of FEs for the modeling of the infinite medium stems precisely from the need to satisfy the Sommerfeld radiation condition. A typical approach for tackling the difficulty consists of truncating the unbounded domain Ω^+ by the introduction of an absorbing (artificial) boundary Γ_a at some distance from the structure (Fig. 1b).

The equation of motion (1) is then solved in the annular region Ω^f which is bounded by the fluid-structure interface Γ and the absorbing boundary Γ_a In order, however, for the resulting problem in Ω^f to be well-posed, an appropriate condition needs to be specified on Γ_a. Towards this end, the following second-order conditions are used [1–4,6] on Γ_a.

In two dimensions,

$$\dot{p}_n + \gamma p_n = -\frac{1}{c}\ddot{p} + \left(\frac{1}{2}\kappa - \frac{\gamma}{c}\right)\dot{p} + \frac{1}{2}cp_{\lambda\lambda} + \left(\frac{1}{8}\kappa^2 c + \frac{1}{2}\kappa\gamma\right)p \tag{2}$$

where n denotes the outward normal to Γ_a, λ denotes the arc-length along Γ_a, κ is the curvature of Γ_a and γ is a stability parameter.

In three dimensions,

$$\dot{p}_n + \gamma p_n = -\frac{1}{c}\ddot{p} + \left(H - \frac{\gamma}{c}\right)\dot{p} + H\gamma p + \frac{c}{2\sqrt{EG}}\left[\left(\sqrt{\frac{G}{E}}p_u\right)_u + \left(\sqrt{\frac{E}{G}}p_v\right)_v\right] + \frac{c}{2}(H^2 - K)p \tag{3}$$

where for the boundary surface Γ_a, n denotes the outward normal, u and v denote the surface parameters, H and K denote the mean and Gaussian curvature, respectively, E and G are the usual coefficients of the first fundamental form, γ is a stability parameter and subscripts denote partial derivatives. In writing Eq. (3), it is assumed that the surface parameters u and v represent orthogonal curvilinear coordinates (e.g. the meridional and polar angles in spherical coordinates).

It can be further shown that, upon introduction of the auxiliary variables $q^{(1)}$ and $q^{(2)}$, Eq. (2) is equivalent to the following set of equations:

$$-p_n = \frac{1}{c}\dot{p} - \frac{\kappa}{2}p - \frac{c}{2\gamma}q^{(1)}_{\lambda\lambda} - \frac{\kappa^2 c}{8\gamma}q^{(2)} \tag{4a}$$

$$p_{\lambda\lambda} - q^{(1)}_{\lambda\lambda} - \frac{1}{\gamma}\dot{q}^{(1)}_{\lambda\lambda} = 0 \tag{4b}$$

$$p - q^{(2)} - \frac{1}{\gamma}\dot{q}^{(2)} = 0 \tag{4c}$$

Similarly, the 3D absorbing boundary condition, Eq. (3), can be decomposed into

$$-p_n = \frac{1}{c}\dot{p} - Hp - \frac{c}{2\gamma}\ell q^{(1)} - \frac{c}{2\gamma}(H^2 - K)q^{(2)} \tag{5a}$$

$$\ell p - \ell q^{(1)} - \frac{1}{\gamma}\ell\dot{q}^{(1)} = 0 \tag{5b}$$

$$p - q^{(2)} - \frac{1}{\gamma}\dot{q}^{(2)} = 0 \tag{5c}$$

where the operator ℓ is defined as

$$\ell\cdot = \frac{1}{\sqrt{EG}}\left[\left(\sqrt{\frac{G}{E}}(\cdot)_u\right)_u + \left(\sqrt{\frac{G}{E}}(\cdot)_v\right)_v\right] \tag{6}$$

Hence, Eq. (1) and either of Eqs. (4a)–(4c) or (5a)–(5c) together with the equation of motion for the structural domain Ω^s and appropriate continuity relations at the fluid-structure interface provide the complete description for the exterior structural acoustics problem.

A set of FE approximations for the quantities on Γ_a such as p, $q^{(1)}$ and $q^{(2)}$ can now be introduced

$$p(x,t) = \varphi_1^{\mathrm{T}}(x)\mathbf{p}_{\Gamma_a}(t), \qquad q^{(1)}(x,t) = \varphi_2^{\mathrm{T}}(x)\mathbf{q}^{(1)}(t), \qquad q^{(2)}(x,t) = \varphi_3^{\mathrm{T}}(x)\mathbf{q}^{(2)}(t) \tag{7}$$

in which, φ_1, φ_2, and φ_3 are vectors of shape functions; $\mathbf{p}_{\Gamma_a}$, $\mathbf{q}^{(1)}$, and $\mathbf{q}^{(2)}$ are unknown nodal values defined over Γ_a. This allows us to derive a pair of symmetric stiffness and damping matrices, which summarily contain the effect of the absorbing boundary on each element on the boundary Γ_a.

3. Implementational details of absorbing elements

The absorbing BEs are developed for arbitrary geometry; indeed, the boundary surface Γ_a need only be convex [1,3,6]. However, based on the success and the experience drawn from early numerical experiments, it is sought to implement the stiffness and damping matrices for a *circular* absorbing boundary in the 2D case and for a *spherical* absorbing boundary in the 3D case. We shall henceforth denote the radius of either the circular or the spherical boundaries by R.

The stability parameter γ, contained in Eqs. (2), (3), (4a)–(4c), and (5a)–(5c), assists in making the conditions stable in the time domain by preventing exponential error growth. Physically, it is equivalent to adding a certain amount of numerical damping into the fluid. In this implementation and for both the 2D and 3D cases, γ is chosen as c/R. For the chosen types of canonical geometry for the absorbing boundary, and for the above value of γ, it can be shown that the present formulations reduce to those derived by Bayliss and Turkel [7]. Moreover, the various curvatures involved in Eqs. (2), (3), (4a)–(4c), and (5a)–(5c) reduce to

$$\kappa = -\frac{1}{R}, \qquad H = -\frac{1}{R}, \qquad K = \frac{1}{R^2} \tag{8}$$

It can be noted from Eq. (8) that $H^2 - K = 0$; this simplifies the 3D element matrices to have only two degrees of freedom (DOF), namely p and $q^{(1)}$. Thus, for standard linear approximations the dimensions of the element stiffness and damping matrices are (1) 6×6 in 2D having 2 nodes per element with 3 DOF per node, (2) 8×8 in 3D having 4 nodes per element with 2 DOF per node, and (3) 4×4 in 2D axisymmetric case having 2 nodes per element with 2 DOF per node. The corresponding element geometry is shown in Fig. 2.

In Eq. (7), $q^{(1)}$ is approximated directly. However, $q^{(1)}$ does not explicitly appear in FE discretizations resulting from either Eqs. (4a)–(4c) or (5a)–(5c), only its derivatives do. Therefore, any approximate solution for $q^{(1)}$ that differs by a constant from the exact solution to $q^{(1)}$ will still satisfy Eqs. (4a)–(4c) or (5a)–(5c); this is equivalent to numerically introducing a rigid-body mode into the fluid on the absorbing boundary that otherwise does not exist. It is thus evident that the resulting global stiffness and damping matrices, if left untreated, will be rank deficient by one. The remedy to the problem is to constrain, at only one node of one element on the absorbing boundary, the DOF corresponding to $q^{(1)}$. The particular value used for constraining $q^{(1)}$ is inconsequential to the results.

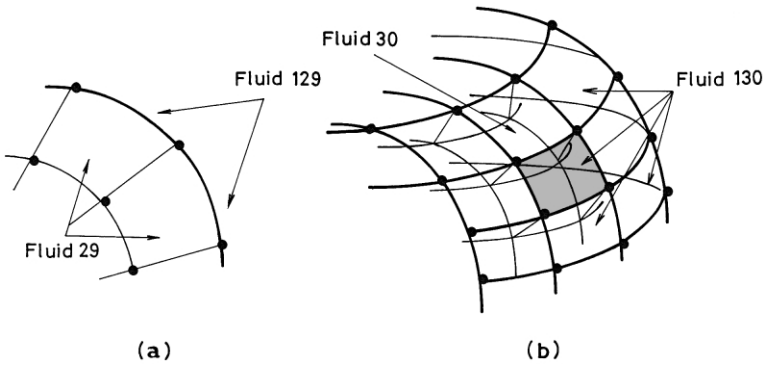

Fig. 2. Typical element geometry. (a) In two dimension; (b) in three dimension.

4. Integral equation to compute far-field pressure

Only time-harmonic problems using the absorbing elements are considered in this paper. In this case, the acoustical pressure is written as $p = P\,e^{j\omega t}$ and as such the wave Eq. (1) reduces to the Helmholtz equation $\nabla^2 P + k^2 P = 0$. P is the pressure amplitude. The solution of the Helmholtz equation for the combined FE system produces the pressure amplitude field in the domain enclosed by Γ_a (Fig. 1b). The pressure amplitude $P(\xi)$ at the point ξ outside Γ_a can now be computed using integral equation

$$P(\xi) = \int_{\Gamma_a} P^*(x,\xi)\frac{\partial P(x)}{\partial n(x)}\,d\Gamma(x) - \int_{\Gamma_a} \frac{\partial P^*(x,\xi)}{\partial n(x)} P(x)\,d\Gamma(x) \tag{9}$$

where $P^*(x,\xi)$ is free-space Green's function for the Helmholtz equation given by

$$\text{2D}: \quad P^*(x,\xi) = \frac{j}{4} H_0^1(kr) \tag{10a}$$

$$\text{3D}: \quad P^*(x,\xi) = \frac{1}{4\pi r} e^{-jkr} \tag{10b}$$

$\mathbf{n}$ is outward normal to Γ_a. $H_0^1(kr)$ is the Hankel function of the first kind and of order zero. k is the wave number $= \omega/c$ and r is the distance between a field point x on Γ_a and a source point ξ outside Γ_a. Note that the computation of $P(\xi)$ requires the pressure gradient $Q_n = \partial P(x)/\partial n$ on Γ_a in addition to the pressure values $P(x)$ on the FE domain boundary. The pressure values are readily available from the FE solution. However, in the FE analysis the pressure gradients are typically computed by differentiating the pressure values. The pressure gradients computed in this fashion are approximate. If these are used in the integral Eq. (9), the resulting pressure values $P(\xi)$ outside Γ_a would contain large errors.

In the FE discretization, the pressure field in an element is a polynomial function, $P(x) = P_j N_j(x)$, where P_j are pressure values at the element nodes and $N_j(x)$ are the associated polynomial shape functions. The normal pressure gradient at the absorbing boundary is computed by taking the dot product of the gradient of pressure and the outward normal $\mathbf{n}$ at the absorbing boundary of the FE domain:

$$\frac{\partial P}{\partial n} = \nabla P \cdot \mathbf{n} \tag{11}$$

In order to evaluate the gradient of pressure at the boundary, the polynomial shape functions are differentiated with respect to the spatial coordinates and evaluated at the boundary of the FE domain:

$$\nabla P = \frac{\partial N_j}{\partial x_j} P_j \tag{12}$$

Therefore, the normal pressure gradient function $\partial P/\partial n$ thus obtained will be one polynomial order lower than that of the pressure field. For example, a linear variation of the pressure field will yield a constant pressure gradient field. When this pressure gradient field is used in evaluating $\partial P/\partial n$ at the boundary nodes, the resulting far field pressures evaluated by the BE integral Eq. (9) will be less accurate.

In order to overcome this deficiency, a novel approach is implemented employing the basic property of the equilibrium of forces in a FE within the FE solution field. That is, instead of obtaining the pressure gradient at the FE absorption boundary by differentiating the pressure field, a direct approach is employed, wherein the following reaction force expression of a FE is employed:

$$Q_i = K_{ij} P_j \tag{13}$$

Accurate pressure gradients at the nodes on the absorbing boundary can be recovered from the reaction flow within the FEs attached to the absorbing elements. This simple procedure is outlined below:

(a) The equilibrium equation within an FE attached to the absorbing boundary is given by

$$[K]\{P\} - \omega^2[M]\{P\} = \{F\} \tag{14}$$

(b) The reactive forces $\{F\}$ or in other words, flows at a node on the absorbing boundary summed for the FEs

attached to the absorbing boundary must equal flow through the node:

$$\sum \{F\}_{\text{at a node}} = Q_n \times \text{Area} \tag{15}$$

(c) The pressure gradient at the node Q_n can now be recovered as follows:

$$Q_n = \frac{\sum \{F\}_{\text{at a node}}}{\text{Area}} \tag{16}$$

For applications in 2D, with the pressure gradients and pressure values thus computed on Γ_a, the accuracy of computation of pressure field values $P(\xi)$ outside Γ_a using Eq. (9) hinges on evaluating Hankel function accurately [8].

The free-space Green's function of Eq. (10a) can also be expressed in terms of Bessel's function as shown below:

$$P^*(x,\xi) = \frac{\mathrm{j}}{4} H_0^1(kr) = \frac{\mathrm{j}}{4}[J_0(kr) + \mathrm{j}Y_0(kr)] \tag{17}$$

The normal derivative of the free-space Green's function, appearing in Eq. (9), can be derived from Eq. (17) as follows:

$$\frac{\partial P^*(x,\xi)}{\partial n(x)} = -\frac{\mathrm{j}k}{4} H_1^1(kr)\frac{\partial r}{\partial n} = -\frac{\mathrm{j}k}{4}[J_1(kr) + \mathrm{j}Y_1(kr)]\frac{\partial r}{\partial n} \tag{18}$$

H_1^1 is the Hankel function of the first kind and first order. J and Y are the Bessel functions of first and second kind. The subscripts 0 and 1 represent the zeroth and first order, respectively. With the help of Eqs. (17) and (18), the integral Eq. (9) for an internal point ξ inside the BE domain, i.e. outside the boundary Γ_a, can be rewritten in terms of Bessel functions:

$$P_R(\xi) = -\frac{1}{4}\int_{\Gamma_a} Y_0(kr) Q_R(x)\mathrm{d}\Gamma(x) - \frac{k}{4}\int_{\Gamma_a} Y_1(kr)\frac{\partial r}{\partial n} \times P_R(x)\mathrm{d}\Gamma(x) \tag{19}$$

$$P_I(\xi) = \frac{1}{4}\int_{\Gamma_a} J_0(kr) Q_I(x)\mathrm{d}\Gamma(x) + \frac{k}{4}\int_{\Gamma_a} J_1(kr)\frac{\partial r}{\partial n} \times P_I(x)\mathrm{d}\Gamma(x) \tag{20}$$

The subscripts R and I stand for the real and the imaginary parts, respectively. The pressure gradient $\partial P(x)/\partial n(x)$ is represented by $Q(x)$. The isoparametric concept of the FE method can be employed to approximate the problem variables $P(x)$ and $Q(x)$, and the geometry in the following fashion:

$$P(x) = \phi_m P_m, \qquad Q(x) = \phi_m Q_m, \qquad S = \phi_m S_m \tag{21}$$

$m = 1, 2$ for linear shape functions. S is the geometry variable along the boundary Γ_a. This approximation for the problem variables $P(x)$ and $Q(x)$ is applicable to the real as well as the imaginary parts. With these approximations, the pressures inside the BE domain outside Γ_a can be computed as

$$P_R(\xi) = -\frac{1}{4}\left\{\int_{\Gamma_a} \phi_m Y_0(kr)\mathrm{d}\Gamma(x)\right\} Q_{Rm} - \frac{k}{4}\left\{\int_{\Gamma_a} \phi_m Y_1(kr)\frac{\partial r}{\partial n}\mathrm{d}\Gamma(x)\right\} P_{Rm} \tag{22}$$

$$P_I(\xi) = \frac{1}{4}\left\{\int_{\Gamma_a} \phi_m J_0(kr)\mathrm{d}\Gamma(x)\right\} Q_{Im} + \frac{k}{4}\left\{\int_{\Gamma_a} \phi_m J_1(kr)\frac{\partial r}{\partial n}\mathrm{d}\Gamma(x)\right\} P_{Im} \tag{23}$$

With the pressure and pressure gradient known on the boundary Γ_a, the pressure field computation in the BE domain outside the boundary Γ_a is posed as a post-processing exercise. The integrals in Eqs. (22) and (23) thus do not involve the evaluation of singular integrals, since the pressure computation is restricted to the domain outside of Γ_a and not including the boundary Γ_a itself. In this case, $r \neq 0$ and the source point ξ never coincides with any of the field points x.

The integration is performed using four Gaussian integration points, which is found to produce solution of adequate accuracy. As mentioned earlier, the accuracy of the computed pressure field depends on the accurate evaluation of Hankel function, i.e. the Bessel functions J and Y. The efficient ways of evaluating Bessel functions, as described by Abramowitz and Stegun [11], are adopted here.

5. Example problems

A number of time-harmonic acoustic scattering problems are illustrated here to demonstrate the accuracy and efficiency of the absorption element and the validity of the procedure of pressure field computation outside the FE domain using integral equation, as outlined above. The absorbing element performs well for low as well as high frequency excitations. It is determined through numerical experiments that the placement of the absorbing elements at a distance of approximately 0.2λ beyond the region occupied by the inclusion or source of vibration is adequate to produce accurate solutions. The first problem presented below deals with pressure wave scattering due to a plane wave traveling from infinity and impinging on a circular rigid cylinder. The second example solves for the scattered pressure due to the vibration of a speaker cone.

5.1. Rigid cylinder impinged by a plane wave

Fig. 3 shows a circular cylindrical inclusion of radius a. A plane harmonic wave $f = \mathrm{e}^{\mathrm{j}kx}$ traveling along x-axis

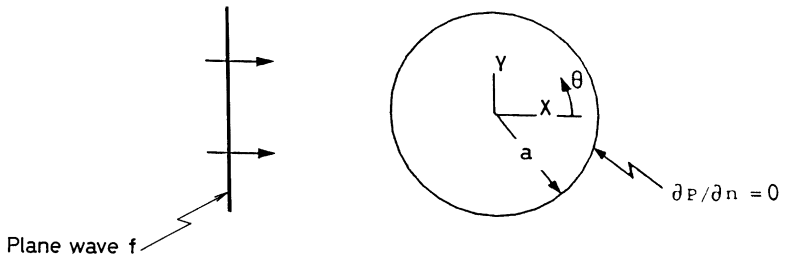

Fig. 3. Rigid cylinder impinged on by a plane wave ($a = 1, f = e^{jk\omega}$).

towards the inclusion is also shown in the figure. The obstacle created by the inclusion would produce scattered pressure wave. The boundary of the cylinder is considered to be rigid, i.e. the normal velocity ($\partial P_t/\partial n$) must equal zero on the cylinder boundary. P_t is the sum of the incident pressure f and the scattered pressure P. As a result, $Q_n = \partial P/\partial n = -\partial f/\partial n$. The radius is taken as $a = 1$. The problem is to predict the scattered pressure field outside the inclusion. Two cases are considered: $k = 1$ and $k = 5$.

Case (i): *Impinging plane wave with a low wave number* $k = 1$. In this case, the wave length is computed as $\lambda = 2\pi$ with $c = 1$. The absorbing elements are placed at $3a$ from the center of the cylindrical inclusion. The circular boundary of the cylinder is divided into 36 segments which would comfortably resolve the wave number of 2π. The absorbing elements are 'glued' to the FE mesh on the outer boundary at $3a$. The problem is solved and then the pressure field outside the computation domain is found using the integral equation. Table 1 shows the scattered pressure solutions at a radius of $r = 5a$ using the current approach and an eigenfunction expansion method, referred to in the paper by Banaugh and Goldsmith [9]. The agreement appears to be good.

Case (ii): *Impinging plane wave with a high wave number* $k = 5$. With the value of the speed of sound taken as $c = 1$, here the wave length is computed as $\lambda = (2\pi/5)$. The absorbing elements are now placed at $2a$ from the center of the cylindrical inclusion. In order to resolve this lower wave number, the mesh density is doubled compared to case (i). As before, the absorbing elements are 'glued' to the outer boundary at $2a$ (Fig. 4). Table 2 shows the scattered pressure solutions at the radius of $r = a$ using the current approach. Note that these solutions are inside the FE domain. The solutions using the eigenfunction expansion method, referred to in Ref. [9] are also shown in the table. The results agree well.

5.2. Vibration of a loudspeaker

A loudspeaker mounted in a box enclosure is considered

Table 1
Rigid cylinder problem

Angle	Current method		Eigenfunction expansion method	
	Real part	Imaginary part	Real part	Imaginary part
0	0.222541	0.129058	0.226	0.132
10	0.214927	0.129393	0.218	0.132
20	0.192706	0.130407	0.195	0.133
30	0.157667	0.132115	0.159	0.135
40	0.112543	0.134516	0.113	0.137
50	0.606897×10^{-1}	0.137570	0.059	0.139
60	0.569874×10^{-2}	0.141169	0.003	0.142
70	-0.489805×10^{-1}	0.145136	−0.053	0.146
80	−0.100371	0.149232	−0.105	0.149
90	−0.146204	0.153194	−0.151	0.153
100	−0.185042	0.156767	−0.189	0.156
110	−0.216288	0.159754	−0.220	0.159
120	−0.240094	0.162041	−0.243	0.161
130	−0.257196	0.163615	−0.259	0.162
140	−0.268708	0.164557	−0.270	0.163
150	−0.275904	0.165014	−0.276	0.163
160	−0.280010	0.165166	−0.279	0.163
170	−0.282034	0.165177	−0.281	0.163
180	−0.282632	0.165167	−0.281	0.163

Pressure solution inside FE domain at $r = 5$ ($k = 1$).

Table 2
Rigid cylinder problem

Angle	Current method		Eigenfunction expansion method	
	Real part	Imaginary part	Real part	Imaginary part
0	−0.67837	1.2684	−0.681	1.231
10	−0.37791	1.2285	−0.382	1.205
20	0.30754	1.0402	0.303	1.046
30	0.88218	0.61775	0.883	0.643
40	0.93641	0.67027×10^{-1}	0.944	0.086
50	0.47936	−0.30670	0.488	−0.310
60	-0.52324×10^{-1}	−0.28261	−0.051	−0.300
70	−0.19184	-0.80694×10^{-2}	−0.199	−0.021
80	0.88322×10^{-1}	0.11233	0.081	0.114
90	0.35564	−0.12783	0.355	−0.118
100	0.21175	−0.48744	0.216	−0.481
110	−0.27896	−0.56379	−0.275	−0.564
120	−0.71473	−0.23306	−0.713	−0.236
130	−0.79611	0.28404	−0.795	0.2820
140	−0.54191	0.70167	−0.540	0.700
150	−0.15885	0.90030	−0.157	0.899
160	0.16968	0.92891	0.171	0.927
170	0.36756	0.89319	0.369	0.890
180	0.43106	0.87228	0.432	0.868

Pressure solution inside FE domain at $r = 1$ ($k = 5$).

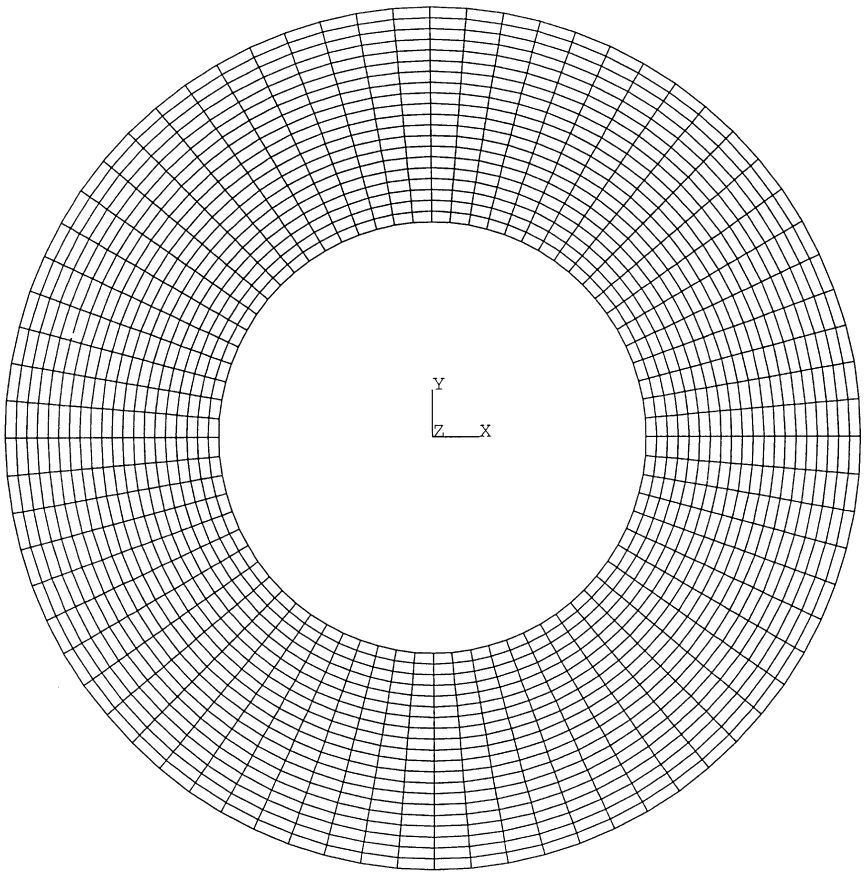

Fig. 4. FE mesh for a rigid cylinder impinged by a plane wave of wave number $k = 5$.

in this study [10]. The speaker box is 1200 mm high and 750 mm wide. The loudspeaker is semi-circular in shape, 5 mm thick and of radius 300 mm. The speaker box is modeled using 2D structural FEs having u_x and u_y DOF, whereas the loudspeaker is modeled using 1D beam elements having u_x, u_y and θ_z DOF. Five nodes located around the center of the cone is subjected to a unit time-harmonic excitation in the x-direction. The objective is to compute sound pressure distribution in the air surrounding the loudspeaker. The speed of sound in the air is taken as 340 m/s. The speaker box cavity is assumed to be a vacuum.

5.2.1. Speaker cone vibration with a frequency of 100 Hz

The speaker cone is excited by a set of forces at a relatively low frequency of 100 Hz. The wave number and the wave length are computed to be $k = 1.85$ and $\lambda = 3400$ mm, respectively. The absorbing elements are placed at a radius of $r = 2000$ mm centered near the middle of the box. The air between the speaker box and the absorbing elements are modeled with 2D acoustic fluid FEs with pressure DOF. The structural FEs of the speaker system is coupled to the acoustic fluid elements. The solution of this system would yield pressure distribution in the air surrounding the speaker box up to a distance of $r = 2000$ mm from the middle of the cone. An annular grid of points is then created up to a distance of $r = 5000$ mm and pressure values are computed using integral equations. The magnitude of pressure in the air is shown in Fig. 5a. Note that the annular gap just outside $r = 2000$ mm indicates the demarcation line between the FE and the integral equation domain.

There is no analytical solution available for this problem and so there is no obvious way to compare the results obtained using the integral equation. Therefore, the problem is re-solved by modeling the entire region between the speaker box and $r = 5000$ mm using the acoustic fluid elements and placing the absorbing elements at $r = 5000$ mm. The magnitude of the pressure is plotted once again and shown in Fig. 5b. The contour plot of Fig. 5a is seen to be identical to that of Fig. 5b demonstrating the good quality of solution produced by the integral equation outside Γ_a.

6. Conclusions

A family of absorbing-boundary FEs is presented for acoustic time-harmonic, transient and modal analyses. These absorbing elements are local and produce banded symmetric matrices. These characteristics make these elements suitable for use in the general-purpose FE program like ANSYS. The absorbing elements are implemented in a user-friendly way in that no additional nodal points need to be defined in order to introduce them into the model. They

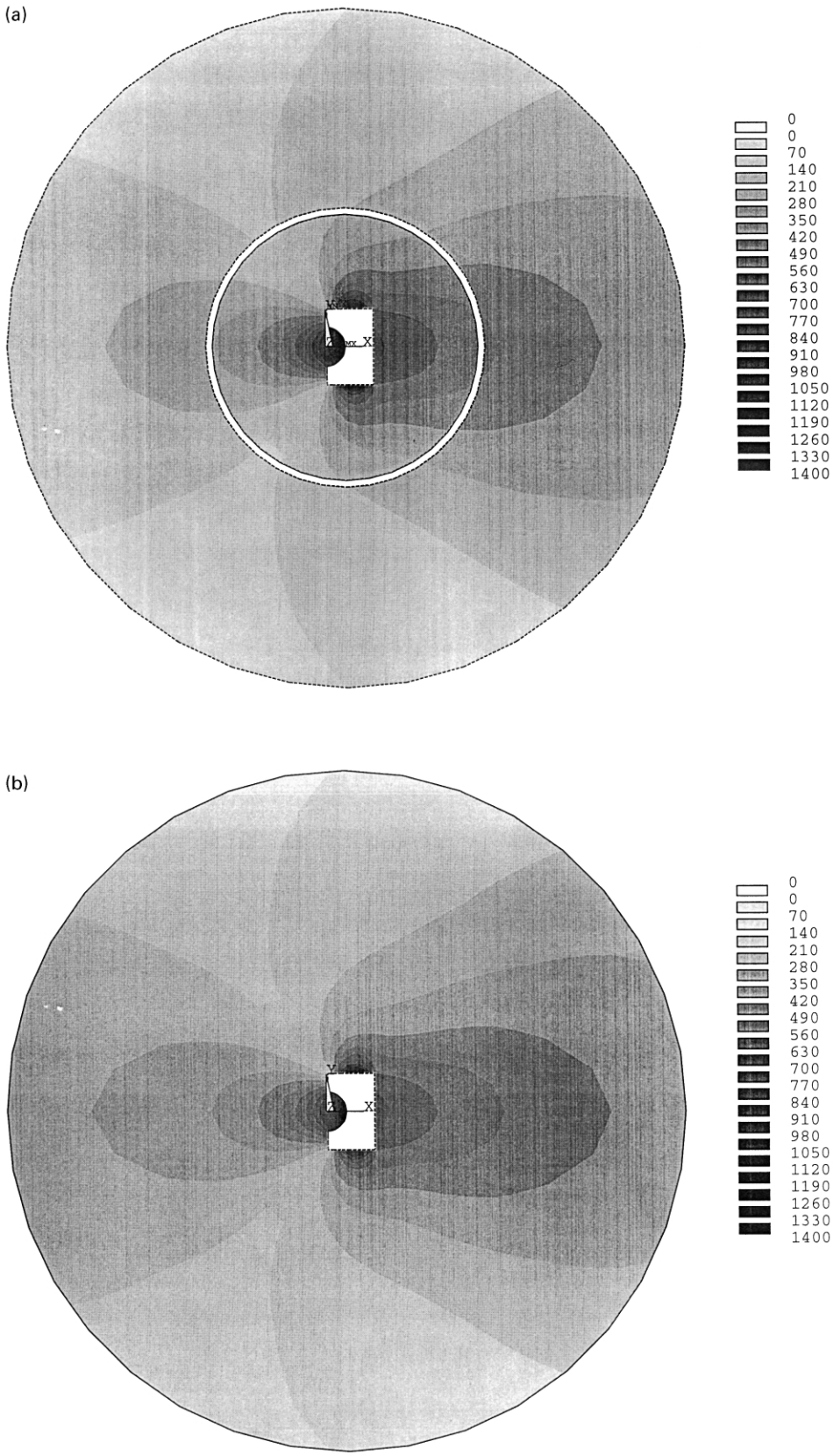

Fig. 5. (a) Pressure magnitude distribution for the coupled speaker–air system for $f = 100$ Hz; (b) pressure magnitude distribution for the coupled speaker–air system for $f = 100$ Hz.

can simply be 'glued' to the prematurely truncated FE mesh. The use of these absorbing elements not only reduce the FE model, but leads to more accurate solutions.

Since the use of the absorbing elements allows premature truncation of the FE mesh, integral equation method is used to compute pressure distribution outside the FE domain. It is shown that, in the case of time-harmonic acoustic analysis, the computation of accurate pressure gradients at the nodes on the absorbing elements is crucial to guarantee a good quality pressure solution in the integral equation domain. The 2D example problems demonstrate the power of the absorbing elements and the usefulness and accuracy of the integral equation method in predicting sound pressure distribution.

Acknowledgements

The authors would like to thank ANSYS, Inc. for providing the opportunity to work on this research. The excellent work of Jackie Williamson and Mini Kora in preparing the manuscript is acknowledged.

References

[1] Kallivokas LF, Bielak J, MacCamy RC. Symmetric local absorbing boundaries in time and space. J Engng Mech 1991;117(9):2027–48.
[2] Kallivokas LF, Bielak J. An element for the analysis of transient exterior fluid-structure interaction problems using the FEM. Finite Elem Anal Des 1993;15:69–81.
[3] Kallivokas LF, Bielak J. Time-domain analysis of transient structural acoustics problems based on the finite element method and a novel absorbing boundary element. J Acoust Soc Am 1993;94(6):3480–92.
[4] Kallivokas LF, Bielak J. A time-domain impedance element for FEA of axisymmetric exterior structural acoustics. ASME J Vib Acoust 1995;117:145–51.
[5] ANSYS User's Manual. Chapter 7. Theory reference, Rev. 5.4; 1997.
[6] Barry A, Bielak J, MacCamy RC. On absorbing boundary conditions for wave propagations. J Comput Phys 1988;79(2):449–68.
[7] Bayliss A, Turkel E. Radiation boundary conditions for wave-like equations. Commun Pure Appl Math 1980;33(6):707–25.
[8] Rajakumar C, Ali A, Yunus SM. A new acoustic interface element for fluid-structure interaction problems. Int J Numer Meth Engng 1992; 33:369–86.
[9] Banaugh RP, Goldsmith W. Diffraction of steady acoustic waves by surfaces of arbitrary shape. J Acoust Soc Am 1963;35(10):1590–601.
[10] Rajakumar C, Ali A. Boundary element–finite element coupled eigen-analysis of fluid-structure systems. Int J Numer Meth Engng 1996;39:1625–34.
[11] Abramowitz M, Stegun IE. Handbook of mathematical functions. US Department of Commerce; 1972. Tenth printing.